Steel and Composite Structures, *Vol. 24, No. 4 (2017) 425-439*
DOI: https://doi.org/10.12989/scs.2017.24.4.425

Static behavior of steel tubular structures considering local joint flexibility

Yamin Wang [1], Yongbo Shao [*1] and Yifang Cao [2]

[1] *School of Mechatronic Engineering, Southwest Petroleum University, Chengdu 610500, P.R. China*
[2] *Center for Infrastructure Engineering, School of Computing, Engineering and Mathematics, Western Sydney University, NSW 2751, Australia*

(*Received January 22, 2017, Revised April 03, 2017, Accepted April 19, 2017*)

Abstract. As a thin-walled structure, local joint flexibility (LJF) in a tubular structure is prominent, and it may produce significant effect on the static performance for the overall structure. This study presents a simplified analytical model to analyze the static behavior for a steel tubular structure with LJF. The presented model simplifies a tubular structure into a frame model consisted of beam elements with considering the LJFs at the connections between any two elements. Theoretical equations of the simplified analytical model are deduced. Through comparison with 3-D finite element results of two typical planar tubular structures consisted of T- and Y-joints respectively, the presented method is proved to be accurate. Furthermore, the effect of LJF on the overall performance of the two tubular structures (including the deflection and the internal forces) is also investigated, and it is found from analyses of internal forces and deformation that a rigid connection assumption in a frame model by using beam elements in finite element analysis can provide unsafe and inaccurate estimation.

Keywords: tubular structure; local joint flexibility (LJF); simplified analytical model; theoretical equations; static behavior

1. Introduction

Tubular structures are commonly used in practical engineering due to many attractive advantages such as light weight, high strength, beautiful appearance and low drag coefficient etc. A typical tubular structure is consisted of different hollow section tubes. The tube members are generally connected together by welding to form a series of joints. In a tubular joint, one or several small tubes (braces) are connected to a big one (chord). The braces are welded directly onto the outer surface of the chord to form a welded tubular joint. In such a tubular joint, the chord member at the connection has to sustain the loading transferred from the braces in its radial direction, which causes the chord wall to be subjected to flexural action. Due to the hollow section of a steel tube, the thin-walled chord has low bending rigidity. In case of no stiffening measures inside the chord wall at the joint location, the chord surface near the brace/chord connection has a significant deformation which can not be ignored in the performance analysis of a tubular structure. API (2000) indicates that the local stiffness around the joint connection has a clear effect on both the displacement and the fatigue life of a tubular structure. For convenience in design stage, the static behavior of a tubular structure is generally simulated initially by spatial frameworks with either rigid joints or completely flexible joints, and the local joint flexibility around the brace/chord connection is not considered. Obviously, the internal forces (including axial force, shear force and bending moment) in each tube member is underestimated if a rigid brace/chord connection is used in the simulation, and this will cause an unsafe design for predicting the loading carrying capacity and serviceability. However, the displacement and the internal forces of each tube member are overestimated if a completely flexible joint connection is used in the simulation, which results in an uneconomical design. Based on these considerations, the local joint stiffness or flexibility is necessary to be taken into account in the design of an unstiffened tubular structure to provide more accurate prediction on the static behavior of welded tubular structures for design purpose.

In the literature, the effect of local connection flexibility on the performance of different structures has been widely investigated. Liu *et al*. (2015) studied the effect of joint rigidity on dome structures. Effect of joint rigidity of beam-column connection on steel frame structures in building engineering was presented by some researchers, and corresponding design and analysis methods were also presented (Sagiroglu and Aydin 2015, Nguyen and Kim 2016). Gou *et al*. (2015) proposed a concept of nominal rigidity for long-span V-shaped rigid frame composite arch bridge, and used this concept to evaluate the rigidity of the arch-to-beam connection.

For tubular structures, Bouwkamp (1966) firstly began to investigate the local joint flexibility (LJF). Later, many researchers studied the LJF effect on the overall performance of tubular structures (Mirtaheri *et al*. 2009, Wang and Chen 2005, Yang *et al*. 1990). It is found from the above investigations that LJF has a significant effect on the static and fatigue behavior of tubular structures. To

*Corresponding author, Professor,
E-mail: cybshao2009@hotmail.com; ybshao@swpu.edu.cn

http://www.techno-press.org/?journal=scs&subpage=6
ISSN: 1229-9367 (Print), 1598-6233 (Online)

consider the effect of LJF, it is necessary to know how to calculate the LJF in a tubular structure. Fessler *et al*. (1986) and Ueda *et al*. (1990) presented some parametric equations for predicting the LJFs of simple tubular joints such as T- and Y-joints. These parametric equations are obtained from curve fitting technique, and they are consisted of material's elastic modulus and some geometrical parameters (chord diameter D, radius-to-thickness ratio of chord γ, brace-to-chord diameter ratio β, and brace-to-chord intersecting angle α). As the LJF reflects the capacity of the chord surface around the brace/chord intersection to resist radial deformation, such capacity is related to the material's stiffness (elastic modulus), the geometrical stiffness (determined by γ and β), and the load component in radial direction (influenced by α). Similar research studies have been conducted by other researchers (Asgarian *et al*. 2014, Gao *et al*. 2013, 2014, Jia and Chen 2014, Qiu and Zhao 2009, Qiu *et al*. 2011) , and parametric equations were also presented for predicting the LJFs of other types of tubular joints.

The above presented parametric equations for predicting the LJFs of different tubular joints are necessary to be introduced into the analyses of the entire tubular structures. Some researchers presented simplified empirical models to analyze the performance of offshore platforms considering the effect of LJFs (Chen *et al*. 1990, Chen and Zhang 1996, Hu *et al*. 1993). In these models, all the tubular members were simplified into beam elements, and the LJFs at both ends of a beam element with an expression of material's elastic modulus and geometrical parameters were incorporated in the stiffness matrix. When different types of tubular joints are analyzed, the stiffness matrix of the beam element has to be modified. Alanjari *et al*. (2011) conducted some research work on presenting nonlinear joint flexibility element for modelling a tubular structure, and a fictious equivalent element was used to simulate the LJF. The difficulty of this method is to determine the reasonable dimension of such equivalent element. The accuracy of this method is not verified through comparison with experimental result.

As the LJF in a tubular structure represents a semi-rigid joint at the brace/chord intersection, the analysis of the entire tubular structure can be carried out by introducing the LJF into the equilibrium equation in finite element method. This study then aims to develop an analytical method for analyzing the static behavior of a tubular structure with consideration for the LJFs. The presented method is implemented based on the premise that the LJFs of different tubular joints in a tubular structure can be calculated easily from the reported parametric equations as mentioned above. The entire tubular structure is then simplified into a frame structure consisted of beam elements. For the beam elements representing the brace members, LJFs are simulated at the brace/chord connections. Using this method, a tubular structure is then simplified into a simple frame structure, and the detailed solving process is introduced. Finally, the accuracy of the presented method is verified through the comparison with 3-D FEA on two typical tubular structures.

2. Analytical method for welded tubular structures considering LJF

2.1 Definition on LJF of a tubular structure

In a welded tubular structure, the chord surface around the weld toe yields local deformation when the brace is subjected to axial loading or bending moment, as shown in Figs. 1(a) and (b). Such deformation causes the brace/chord connection to be not rigid, and it may produce significant effect on the static behavior of the structure. The local joint flexibility (LJF) is then proposed to describe this phenomenon.

As shown in Figs. 1(a) and (b), C1 and C2 are located at the crown, and S1 and S2 are the saddles. In case of an axial loading at the brace end, as shown in Fig. 1(a), the joint has a local deformation in the brace axial direction, which produces an axial LJF. It is assumed that the displacements at the four critical positions in the brace axial direction are denoted by u_{c1}, u_{c2}, u_{s1} and u_{s2}. The axial displacement of the brace at the intersection u_b is then defined as the average value of the displacements at such four points as follow

$$u_b = \frac{u_{c1} + u_{c2} + u_{s1} + u_{s2}}{4} \tag{1}$$

Two locations which are located at two sides of the chord and coincide with the intersecting point of two axes of the brace and the chord in the direction perpendicular to the joint plane (namely a_1 and a_2), as shown in Fig. 1, are selected to define the displacement of the chord u_c as follow

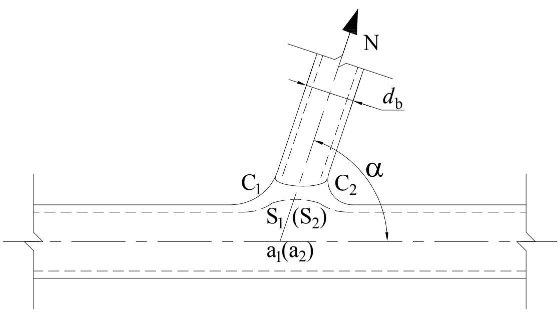

(a) Axial loading

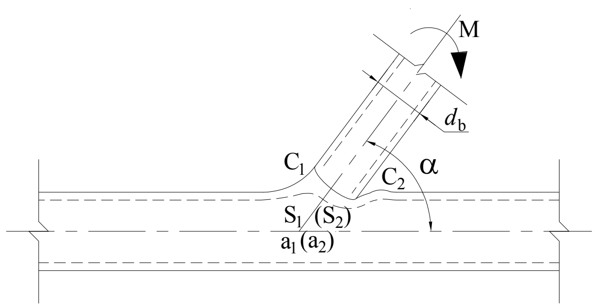

(b) Bending moment

Fig. 1 Local deformation at brace/chord intersection of a tubular joint

$$u_c = \frac{u_{a1} + u_{a2}}{2} \tag{2}$$

The axial deformation u_R at the joint due to LJF is calculated from the following equation

$$u_R = u_b - u_c \tag{3}$$

If an axial load N is applied at the brace end, the axial LJF, namely LJF_n, is defined by the following equation

$$LJF_n = \frac{u_R}{N} \tag{4}$$

Accordingly, the local axial stiffness at the joint, namely k_n, is calculated directly from LJF_n as follow

$$k_n = \frac{1}{LJF_n} = \frac{N}{u_R} \tag{5}$$

Eqs. (1)-(5) provide the method for calculating the local axial flexibility and stiffness at the joint. For a tubular joint under in-plane bending moment M, as shown in Fig. 1(b), the rotating angle θ_R at the intersection is calculated from the following equation

$$\theta_R = \arctan\left[\frac{(u_{c1} - u_{c2})\sin\alpha}{d_b}\right] \approx \frac{(u_{c1} - u_{c2})\sin\alpha}{d_b} \tag{6}$$

where α is the intersecting angle between the brace and the chord as shown in Fig. 1, and d_b is the diameter of the brace.

The local rotating flexibility and stiffness at the joint due to bending moment, denoted by LJF_m and k_m respectively, are calculated from the following two equations

$$LJF_m = \frac{\theta_R}{M} \tag{7}$$

$$k_m = \frac{1}{LJF_m} = \frac{M}{\theta_R} \tag{8}$$

2.2 Simplified analytical model for LJF of a tubular joint

As the LJF of a tubular structure is mainly focused on the brace/chord connection, the most accurate simulating method is to carry out 3-D finite element analysis because such method can consider the complicated geometry at the joint position. In a 3-D finite element analysis, the mostly common scheme for discretizing the tubular joint is using brick elements or shell elements to generate the structural mesh. However, a big problem may occur when a tubular structure is consisted of many tube members because a huge number of elements are necessary to complete the finite element mesh of the entire structure. To obtain an accurate and convergent result, more than several thousands of elements may be required in even a simple tubular T- or Y-joint, and the computing efficiency is a big problem in case that so many nodes in the mesh of the structure are necessary. To solve this problem, a simplified analytical model for analyzing a tubular joint with LJF is presented. This simplified analytical model aims to improve the computing efficiency through reducing the number of elements in the mesh. A simple alternative is to replace the 3-D brick elements with beam elements since a single beam element can be used to model an entire tube member. At the connection between a brace and a chord, in which position LJF exists, some special measures are taken into account. The simplified analytical model is referred to component based method, and it can be illustrated in Fig. 2 which shows a simple tubular joint consisted of a chord and a brace. In the component based method, the chord and the brace are both simplified as beam elements. The chord is divided into two beam elements which are connected at the joint position. The two beam elements are rigidly connected and there is no local flexibility at the connection between them. The beam element used to model the brace member, however, has local flexibility at the connection to the chord, and the end of the brace connecting to the chord may deviate from the chord axis and rotate about the brace/chord connection. To simulate such LJFs, two equivalent springs can be used as shown in Fig. 2. An axial spring can simulate the local axial deformation, and the torsional spring is used to simulate the rotating deformation. In theory, the stiffness of the axial spring and the stiffness of the torsional spring denoted with k_n and k_m respectively are calculated from Eqs. (5) and (8) respectively.

Using the simplified analytical model in Fig. 2, a tubular structure is then equivalent to a frame consisted of beam elements and special joints. It is noted here that the connection between two chord members can be also simulated with the above two springs only by considering a

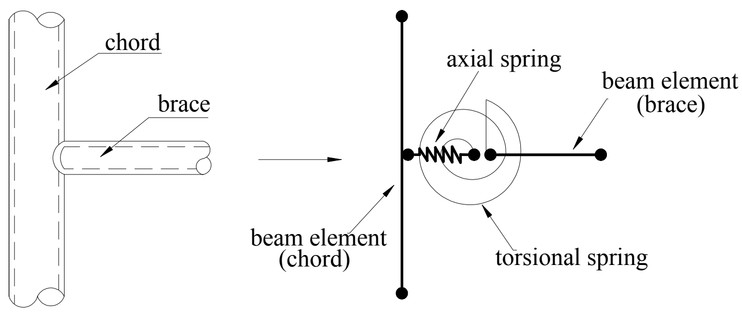

Fig. 2 Simplified analytical model for a tubular joint

very large value of k_m and k_n. It is clear that each tube in a tubular structure can be modelled by only one beam element in the simplified analytical model and no 3-D simulation is necessary. Such treatment can shorten the computing time greatly and provides a quick calculation. However, the simplified analytical model needs a reliable estimation for the LJF at any joint. Fortunately, many parametric equations have been presented in the literature for calculating the LJFs of different types of tubular joints such tubular T-, Y- and K-joints (Alanjari *et al.* 2011, Fessler *et al.* 1986, Ueda *et al.* 1990), tubular X-joints (Qiu and Zhao 2009, Qiu *et al.* 2011), and completely overlapped tubular joints (Gao *et al.* 2013, 2014). All these parametric equations are expressed with material's elastic modulus and some key geometrical parameters (i.e., D, γ, β, α and so on). Detailed expression of these parametric equations can be found in the listed corresponding references. In addition, the LJF of a tubular joint can be also obtained from finite element analysis or experimental test directly. Once the values of the LJFs are determined, a tubular structure can be analyzed from finite element method based on a combination of the conventional beam elements and the introduced LJF.

2.3 Axial LJF in a tubular joint

As each tube member in a tubular structure has two ends, two local flexibility coefficients are considered in the simplified beam element. Considering a typical tubular structure in Fig. 3, the length of the brace member is assumed to be l, and the distance between two chord axes is l'. A' and B' are two points located on the axes of the two chord members, and A and B are two ends of the brace. It is clear from Fig. 3 that the relationship between the above two quantities is easily expressed as follow

$$l' = l + d_c \tag{9}$$

where d_c is the chord diameter.

In this study, it is assumed that the chord diameter is much smaller than the brace length. It means the following two relationships are satisfied: (1) $l >> d_c$; and (2) $l \approx l'$. When l is not much bigger than d_c, l is replaced by l' to represent the length of the brace.

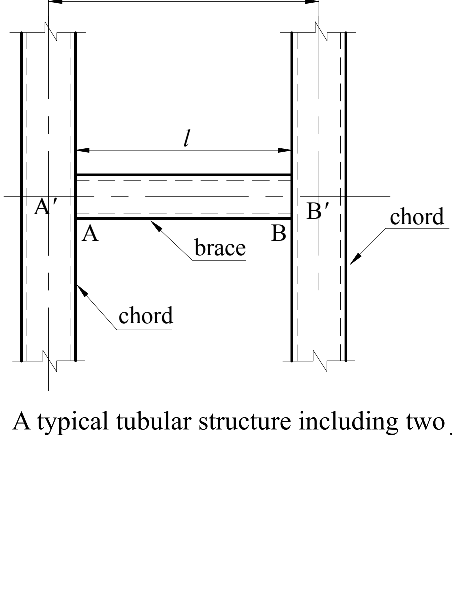

Fig. 3 A typical tubular structure including two joints

If there is no LJF at the brace/chord connection, the tubular structure shown in Fig. 3 is simplified into a conventional rigid frame structure. The displacements of points A' and A are identical. Considering LJF in axial direction of the brace/chord connection, for example, the left joint in Fig. 3, the displacements of the brace end and the chord axis (u_A and $u_{A'}$) are not same (as seen from Fig. 4). There is a relatively displacement u_{RA}, and u_{RA} represents the axial LJF. The relationship between the displacements and the axial forces at both ends of the brace is easily obtained as follow based on previous studies

$$\frac{EA/l}{1+\dfrac{EA/l}{k_{nA}}+\dfrac{EA/l}{k_{nB}}}\begin{bmatrix}1 & -1\\ -1 & 1\end{bmatrix}\begin{Bmatrix}u_A\\ u_B\end{Bmatrix}=\begin{Bmatrix}N_A\\ N_B\end{Bmatrix} \tag{10}$$

or

$$\frac{1}{1+\gamma_{nA}+\gamma_{nB}}\times\frac{EA}{l}\begin{bmatrix}1 & -1\\ -1 & 1\end{bmatrix}\begin{Bmatrix}u_A\\ u_B\end{Bmatrix}=\begin{Bmatrix}N_A\\ N_B\end{Bmatrix} \tag{11}$$

where E and A are the elastic modulus of the materials and the area of the cross section for the brace; N_A and N_B are the axial forces at two ends of the brace. k_{nA} and k_{nB} are local joint stiffness at two ends of the brace in axial direction; LJF_{nA} and LJF_{nB} are corresponding local joint flexibility at two ends. γ_{nA} and γ_{nB} in Eq. (11) are the ratios of the axial stiffness of the brace per unit length to the local axial stiffness at the brace/chord connection, i.e., $\gamma_{nA}=\dfrac{EA/l}{k_{nA}}$ and $\gamma_{nB}=\dfrac{EA/l}{k_{nB}}$. In case of a rigid connection between any two members, $k_n \to +\infty$ and $\gamma_n \to 0$.

2.4 Bending LJF in a tubular joint

In case that the brace member in Fig. 3 is subjected to bending moment at two ends, rotating LJF is necessary to be considered because a rotation between the brace and the chord may occur easily when the LJF at the brace/chord connection is big and the bending moments at the brace/chord connections exist. The bending moment at the brace/chord connection initiates due to two conditions when the brace member is not subjected to any lateral external loading along its length: (1) the chord has a rotating

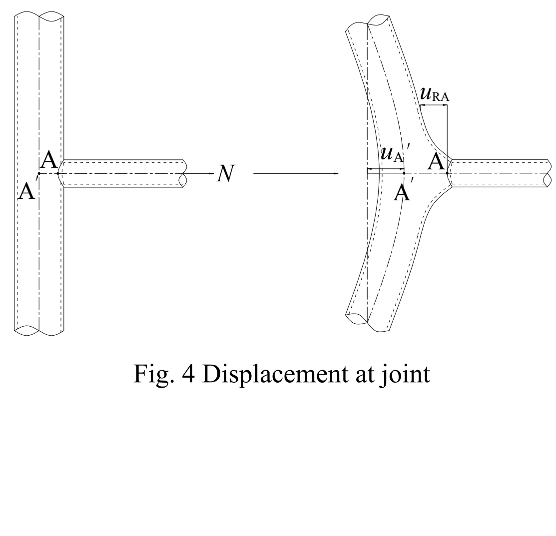

Fig. 4 Displacement at joint

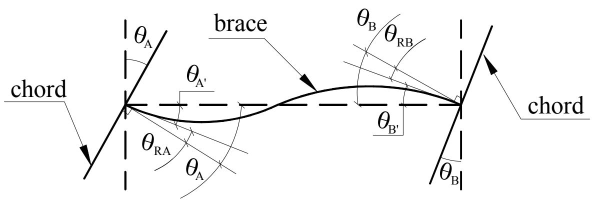

Fig. 5 Rotating deformation at joints

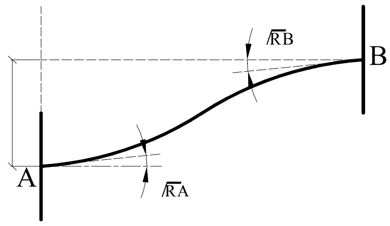

Fig. 6 Relative lateral displacement between two joints

deformation; (2) the two ends of the brace have a relative lateral displacement. In case of a rotating deformation of the chords in the first condition, as the simplified analytical model shown in Fig. 5, the brace rotates about an angle of $\theta_{A'}$ or $\theta_{B'}$ at either connection when the chord has a rotating angle of θ_A or θ_B at the same connection. Due to the LJF at the connection, it is clear that $\theta_{A'} < \theta_{A'} < \theta_A$ and $\theta_{B'} < \theta_B$. The rotating angle between the brace and the chord due to LJF is θ_{RA} at the left brace/chord connection and θ_{RB} at the right brace/chord connection. Clearly, the following relationship can be obtained

$$\begin{cases} \theta_{A'} = \theta_A - \theta_{RA} \\ \theta_{B'} = \theta_B - \theta_{RB} \end{cases} \tag{12}$$

As θ_{RA} and θ_{RB} are caused by the bending moment, they can be calculated based on the definition of the LJF_m as follow

$$\begin{cases} \theta_{RA} = \dfrac{M_A^\theta}{k_{mA}} = M_A^\theta \cdot LJF_{mA} \\ \theta_{RB} = \dfrac{M_B^\theta}{k_{mB}} = M_B^\theta \cdot LJF_{mB} \end{cases} \tag{13}$$

where M_A^θ and M_B^θ are the bending moments at two connections due to chord rotation; k_{mA} and k_{mB} are local joint bending stiffnesses; and LJF_{mA} and LJF_{mB} are local joint bending flexibilities.

According to the fundamentals of structural mechanics, the bending moments at the two connections are determined by the actual rotating angles between the chord and the brace as follow

$$\begin{cases} M_A^\theta = \dfrac{4EI}{l}\theta_{A'} + \dfrac{2EI}{l}\theta_{B'} \\ M_B^\theta = \dfrac{2EI}{l}\theta_{A'} + \dfrac{4EI}{l}\theta_{B'} \end{cases} \tag{14}$$

Substitute Eq. (12) into Eq. (14), the bending moments at the connections are determined by the rotating angles from the following equations

$$\begin{cases} M_A^\theta = \dfrac{4EI}{l}(\theta_A - \theta_{RA}) + \dfrac{2EI}{l}(\theta_B - \theta_{RB}) \\ M_B^\theta = \dfrac{2EI}{l}(\theta_A - \theta_{RA}) + \dfrac{4EI}{l}(\theta_B - \theta_{RB}) \end{cases} \tag{15}$$

Another mechanism to produce bending moment at the brace/chord connection is a relative lateral displacement between the two connections, as shown in Fig. 6. Considering the LJF, there is a rotating angle at the brace/chord connection (θ_{RA} at the left end and θ_{RB} at the right end). Therefore, the simplified model in Fig. 6 is equivalent to a superposition of two deforming mechanisms as shown in Figs. 7(a) and 7(b).

Similarly, the bending moments at the two connections in Fig. 6, M_A^Δ and M_B^Δ, can be easily obtained from the superposition method as follow

$$\begin{cases} M_A^\Delta = \dfrac{6EI}{l^2}(w_A - w_B) - \left(\dfrac{4EI}{l}\theta_{RA} + \dfrac{2EI}{l}\theta_{RB}\right) \\ M_B^\Delta = \dfrac{6EI}{l^2}(w_A - w_B) - \left(\dfrac{2EI}{l}\theta_{RA} + \dfrac{4EI}{l}\theta_{RB}\right) \end{cases} \tag{16}$$

where w_A and w_B are lateral displacements at the two connections.

Obviously, the final bending moments at the two brace/chord connections, M_A and M_B, are the superposition of the corresponding bending moments calculated from Eqs. (15) and (16), and they can be expressed as follow

$$\begin{cases} M_A = M_A^\theta + M_A^\Delta \\ M_B = M_B^\theta + M_B^\Delta \end{cases} \tag{17}$$

Substitute Eq. (13) into Eq. (17), the following equation can be obtained after some simplifications

(a) Rotating angle (b) Relative lateral displacement

Fig. 7 Two deforming mechanisms

$$\begin{cases} M_A = \dfrac{EI}{l}\left(r_{ii}\theta_A + r_{ij}\theta_B\right) + \dfrac{EI}{l^2}\left(r_{ii} + r_{ij}\right)\left(w_A - w_B\right) \\ M_B = \dfrac{EI}{l}\left(r_{ij}\theta_A + r_{jj}\theta_B\right) + \dfrac{EI}{l^2}\left(r_{ij} + r_{jj}\right)\left(w_A - w_B\right) \end{cases} \tag{18}$$

where

$$r_{ii} = \left(4 + \frac{24EI/l}{k_{mB}}\right)\Big/ r_{AB} = \left(4 + 24\gamma_{mB}\right)\Big/ r_{AB}$$

$$r_{jj} = \left(4 + \frac{24EI/l}{k_{mA}}\right)\Big/ r_{AB} = \left(4 + 24\gamma_{mA}\right)\Big/ r_{AB}$$

$$r_{ij} = 2\big/ r_{AB}$$

Based on Eq. (18), the shear forces at the two connections can be easily obtained from the following equation

$$\begin{cases} Q_A = \dfrac{M_A + M_B}{l} = \dfrac{EI}{l^2}\left[\left(r_{ii} + r_{ij}\right)\theta_A + \left(r_{ij} + r_{jj}\right)\theta_B\right] \\ \quad + \dfrac{EI}{l^3}\left(r_{ii} + 2r_{ij} + r_{jj}\right)\left(w_A - w_B\right) \\ Q_B = -Q_A \end{cases} \tag{19}$$

Combining Eqs. (18) and (19), the final following equation is given

$$\frac{EI}{l}\begin{bmatrix} \dfrac{r_{ii}+2r_{ij}+r_{jj}}{l^2} & \dfrac{r_{ii}+r_{ij}}{l} & -\dfrac{r_{ii}+2r_{ij}+r_{jj}}{l^2} & \dfrac{r_{ij}+r_{jj}}{l} \\ & r_{ii} & -\dfrac{r_{ii}+r_{ij}}{l} & r_{ij} \\ & SYM & \dfrac{r_{ii}+2r_{ij}+r_{jj}}{l^2} & -\dfrac{r_{ij}+r_{jj}}{l} \\ & & & r_{jj} \end{bmatrix}\begin{Bmatrix} w_A \\ \theta_A \\ w_B \\ \theta_B \end{Bmatrix} = \begin{Bmatrix} Q_A \\ M_A \\ Q_B \\ M_B \end{Bmatrix} \tag{20}$$

In Eq. (20), SYM denotes symmetrical, and this equation provides the method for solving a tubular structure considering LJF due to bending moment at brace/chord connections.

2.5 Analytical model of a tubular joint considering LJFs

If both axial and flexural LJFs are considered, the governing equation is derived from a combination of Eq. (11) and Eq. (20), and it is expressed as follow

$$[K]^e [a]^e = [F]^e \tag{21}$$

where $[K]^e$ denotes the stiffness matrix of a simplified analytical beam element and it is a symmetrical matrix, i.e., $k_{ij} = k_{ji}$; $[a]^e$ is the displacement matrix at two ends of a simplified beam element; $[F]^e$ is external loading matrix at two ends of a simplified beam element. The detailed expression of each matrix is given as follows

$$[K]^e = \begin{bmatrix} k_{11} & 0 & 0 & k_{14} & 0 & 0 \\ & k_{22} & k_{23} & 0 & k_{25} & k_{26} \\ & & k_{33} & 0 & k_{35} & k_{36} \\ & & & k_{44} & 0 & 0 \\ & SYM & & & k_{55} & k_{56} \\ & & & & & k_{66} \end{bmatrix}$$

$$k_{11} = \frac{EA}{l}\left(\frac{1}{1 + \gamma_{nA} + \gamma_{nB}}\right)$$

$$k_{14} = -k_{11}$$

$$k_{22} = \frac{EI}{l^3}\left(r_{ii} + 2r_{ij} + r_{jj}\right)$$

$$k_{23} = \frac{EI}{l^2}\left(r_{ii} + r_{ij}\right)$$

$$k_{25} = -k_{22}$$

$$k_{26} = \frac{EI}{l^2}\left(r_{ij} + r_{jj}\right)$$

$$k_{33} = \frac{EI}{l} r_{ii}$$

$$k_{35} = -k_{23}$$

$$k_{36} = \frac{EI}{l} r_{ij}$$

$$k_{44} = k_{11}$$

$$k_{55} = k_{22}$$

$$k_{56} = -k_{26}$$

$$k_{66} = \frac{EI}{l} r_{jj}$$

$$[a]^e = \{u_A \ w_A \ \theta_A \ u_B \ w_B \ \theta_B\}^T$$

$$[F]^e = \{N_A \ Q_A \ M_A \ N_B \ Q_B \ M_B\}^T$$

Eq. (21) provides the detailed format of the stiffness matrix of each tube member considering the LJFs. However, such stiffness is obtained based on the assumption that coordinate system is placed along the axis of the simplified beam element. In a tubular structure including many tube members, the axial directions of some tube members are definitely different. In this case, global and local coordinate systems are defined separately as shown in Fig. 8. *x′oy′* in Fig. 8 is a local coordinate system in which the axis of the simplified beam element is placed in the same direction as the *x′*-axis, and *xoy* is a global coordinate system. It is assumed that the local coordinate system is coincided with the global coordinate system if the later one is rotating with an angle of φ in anti-clockwise direction.

The relationship of the stiffness matrix between the global and the local coordinate systems is easily obtained as follow

$$[K]_g^e = [\lambda]^T [K]^e [\lambda] \tag{22}$$

where $[K]_g^e$ is the stiffness matrix of the simplified beam element in global coordinate system.

In Eq. (22), $[\lambda]$, which is a transfer matrix between global and local coordinate systems, is expressed as follow

$$[\lambda] = \begin{bmatrix} \cos\varphi & \sin\varphi & 0 & 0 & 0 & 0 \\ -\sin\varphi & \cos\varphi & 0 & 0 & 0 & 0 \\ 0 & 0 & 1 & 0 & 0 & 0 \\ 0 & 0 & 0 & \cos\varphi & \sin\varphi & 0 \\ 0 & 0 & 0 & -\sin\varphi & \cos\varphi & 0 \\ 0 & 0 & 0 & 0 & 0 & 1 \end{bmatrix} \tag{23}$$

$[\lambda]^T$ in Eq. (22) is the transposed matrix of $[\lambda]$.

In a welded tubular structure, the stiffness matrix of each simplified beam element in global coordinate system can be calculated from Eq. (22). The stiffness matrix of the entire structure is then obtained by superposing the $[K]_g^e$ of all tube members, and the final equation for analyzing the entire structure is formed as follow

$$[K][a] = [F] \tag{24}$$

where $[K]$ is the stiffness matrix of the entire structure, $[a]$ is the displacement matrix of all the nodes, $[F]$ is the external loadings applied at the nodes.

After introducing the boundary conditions at some nodes with constraints, Eq. (24) can be solved from fundamental methods such as Gauss elimination. In this study, a computer-aided program for solving tubular structures considering the LJF is coded by using Fortran based on the presented analytical model, and this program is used to analyze the linear and elastic behavior of tubular structures.

3. Evaluation on presented analytical model

To verify the accuracy and reliability of the above presented method in this study, two cantilevered welded tubular structures as shown in Figs. 9(a) and (b) are studied. In Fig. 9(a), the cantilevered tubular structure is consisted of two chords and three vertical braces. The top and the bottom chords have a diameter of 219 mm and a thickness of 6 mm. For the three braces, the diameter and the thickness are 119 mm and 6 mm respectively. The length of the chords and the braces are also given in Fig. 9(a). The chords and the braces are made of same steel materials with an elastic modulus of E = 206×10^3 N/mm^2 and a Poisson's ratio of 0.3 respectively. At the right end, a steel plate is welded to the top and to the bottom chords. This steel plate is assumed to be rigid by setting a very big value of elastic modulus E = 206×10^6 N/mm^2 and a thickness of 60 mm which can ensure an enough large flexural stiffness compared to the tube members. A concentrated force of 10 kN is applied at the steel plate in downward direction. Clearly, the tubular structure in Fig. 9(a) is only consisted of tubular T-joints in which a brace member is perpendicularly welded to the chord member. The tubular structure in Fig. 9(b) includes two chords and four inclined braces. The chord and the brace members are same as those in Fig. 9(a) both in geometry and in material properties. A same steel plate is also connected to the top and the bottom chords, and a same concentrated force of 10 kN is applied at the plate. However, the tubular structure in Fig. 9(b) is consisted of tubular Y-joints with an inclined angle of 75° at the brace/chord connections.

3.1 Calculation for LJFs of tubular T- and Y-joints

As mentioned previously, the LJF values in a tubular structure are necessary known before using the presented simplified analytical model to carry out analysis. To calculate the LJFs at a tubular joint, three different methods can be used: (1) experimental test; (2) 3-D finite element analysis by using brick elements to discretizing the entire structure; and (3) parametric equations. The first method is generally expensive and time consuming although it can provide most accurate and convincing results. The second

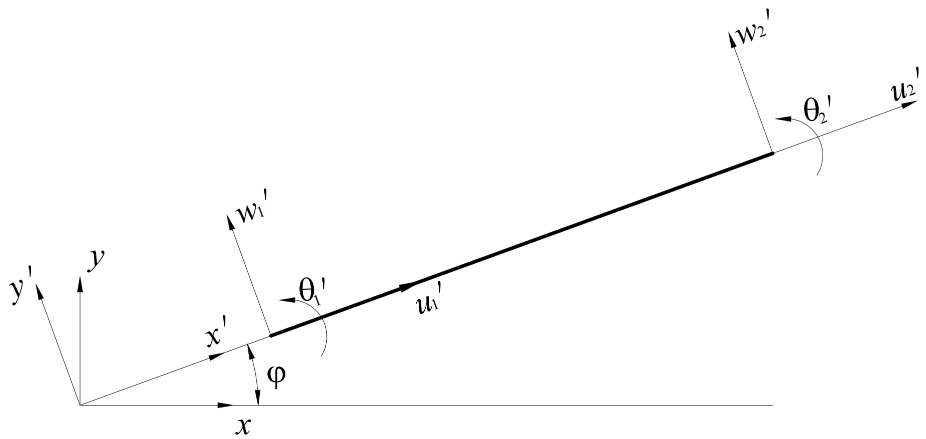

Fig. 8 Global and local coordinate systems

method is more efficient and it is an effective alternative compared to the experimental testing method once its reliability is validated through benchmark verification. The third method, although its accuracy may be the most inaccurate, is a favourite method for design purpose in practical engineering because it can provide a very fast estimation. The parametric equation in the third method is based on the results of experimental tests or finite element analyses for a lot of different tubular joint models. It is generally obtained from curve fitting technique and expressed in the format of some geometrical parameters and material constants. For example, Fessler *et al*. (1986) presented the parametric equations for calculating the LJFs of a tubular T/Y-joint under brace axial load (LJF_n) and in-plane bending moment (LJF_m) as follows

$$LJF_n = \frac{1.95\gamma^{2.15}(1-\beta)^{1.3}\sin^{2.19}\alpha}{ED} \tag{25}$$

$$LJF_m = \frac{134\gamma^{1.73}e^{-4.52\beta}\sin^{1.22}\alpha}{ED^3} \tag{26}$$

Ueda *et al*. (1990) also provided parametric equation for estimating the LJFs of a tubular T/Y-joint from the following equations

$$LJF_n = \frac{0.313\gamma^{2.3}\beta^{-1.2}\sin^2\alpha}{ED} \tag{27}$$

$$LJF_m = \frac{4.22\gamma^{1.7}\beta^{-2.2}\sin\alpha}{ED^3} \tag{28}$$

In Eqs. (25)-(28), γ, β and α are normalized geometrical parameters of a tubular T/Y joint. D is the chord diameter, and E is the elastic modulus of the steel materials. For the normalized geometrical parameters, γ is a ratio of the chord radius to the chord thickness. β is a ratio of the brace diameter to the chord diameter. α is the intersecting angle between the brace and the chord.

For a comparison and evaluation purpose, the T-joint and the Y-joint of the tubular structures in Figs. 9(a) and (b) are selected for discussion. Both finite element analyses and prediction from parametric equations in Eqs. (25)-(28) are carried out. As the finite element technique for analyzing a tubular joint in the literature is quite mature, the details of the finite element model of a tubular T/Y joint are not introduced in this study. In the finite element analyses, the T/Y-joint is fixed at two ends of the chord, and an axial load or an in-plane bending moment is applied at the brace end. Solid element (hexahedral) is used to discretize the entire structure. Finite element software ABAQUS is used to conduct the numerical analyses. The applied axial load or the in-plane bending moment has an appropriate value to ensure that the tubular joint is in linear and elastic stage. Figs. 10(a) and (b) show the mesh of the joints used in the finite element analyses.

The calculated results of the local joint stiffness (inverse of the LJF) both from finite element analyses and from

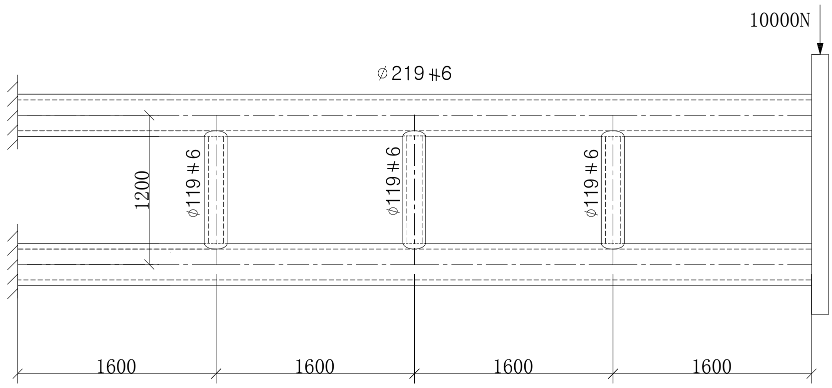

(a) Vertical braces

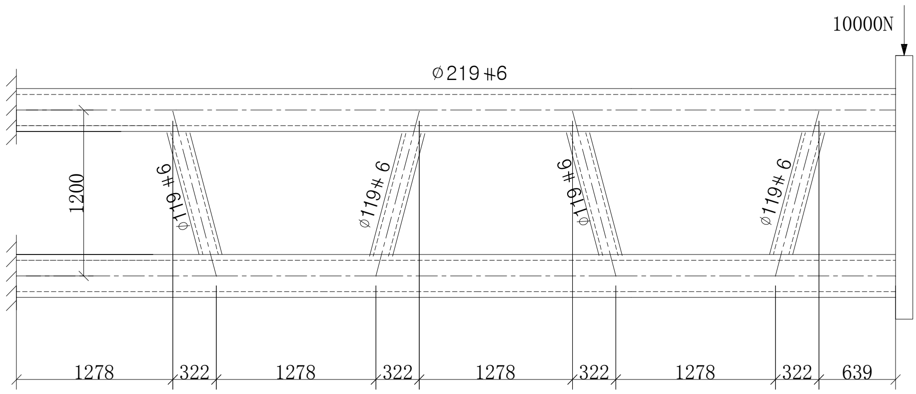

(b) Inclined braces

Fig. 9 Cantilever tubular structures

parametric equations are tabulated in Table 1. AX and IPB denote axial load and in-plane bending moment respectively. k_{FE}, k_{Fl} and k_{Ud} are the LJSs calculated from finite element analyses, Fessler's equation (Eqs. (25)-(26)), and Ueda's equation (Eqs. (27)-(28)) respectively. For comparison, all the predicted results from parametric equations are evaluated from a ratio of the predicted value to the finite element result. The finite element result is assumed to be accurate because such modelling technique has been proved to be reliable in many published research papers. From the tabulated results in Table 1, it is found that Fessler's equation generally overestimates the local joint stiffness. Accordingly, Ueda's equation provides a conservative yet safe estimation for the local joint stiffness of the T/Y-joint because the predicted LJFs from this equation are smaller than the finite element results. In the following study, both finite element results and predicted results from Fessler's equations and Ueda's equations of the LJFs are used in the analyses through the presented simplified analytical model in the following sessions.

3.2 Deformation analysis

Considering the tubular structures in Figs. 9(a) and (b), four different methods are used in the linear and elastic static analyses as illustrated in Figs. 11-12. Figs. 11(a) and 12(a) show 3-D models by discretizing the entire structure with hexahedral elements. These models can simulate the details of both the tube members and the connections. Figs. 11(b) and 12(b) show simplified frame models in which the connections between any two members are rigid and there is no rotation between any two members. In Figs. 11(c) and 12(c), the vertical and the inclined brace tubes are simplified to be hinged to the top and the bottom chord tubes. The simplified brace members between the top and the bottom members are connected to the two chords with LJF as shown in Figs. 11(d) and 12(d). Among the four models, the 3-D finite element model can certainly provide most accurate result in analyzing the static performance of the tubular structures because it considers any geometrical detail. However, a large amount of elements are necessary to generate the mesh in the finite element analysis, which brings difficulty both in computing efficiency and in mesh quality due to the complex geometry around the brace/chord intersection. The simplified models in Figs. 11(b)-(d) and 12(b)-(d) are used to analyze the actual tubular structure in a quite simple way because each tube is replaced by only a beam element or a truss element (brace tubes in Figs. 11(c) and 12(c)). The tubular structure shown in Fig. 9(a) is simplified into a frame model with 12 beam elements in Figs. 11(b) and (d). Accordingly, the tubular structure in Fig. 9(b) is simplified into a frame model with 15 beam elements as shown in Figs. 12(b) and (d). In Figs. 11(c) and 12(c), the tubular structure is simplified into a structure consisted of beam elements (top and bottom tubes and end plate) and truss elements (brace tubes between the top and the bottom chord tubes). It is noted here that the simplified rigid frame models in Figs. 11(b) and 12(b) are usually used

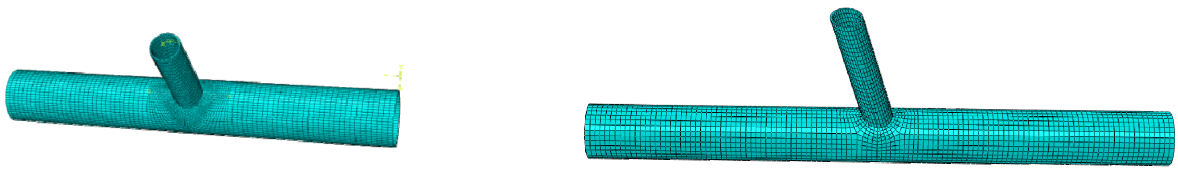

(a) T-joint (b) T-joint

Fig. 10 Finite element meshes of T- and Y-joints

Table 1 Local joint stiffness of T- and Y-joints

Joint type	Loading type	Finite Element (FE) result		Fessler's Equation		Ueda's Equation	
T-joint	AX	LJS k_{FE} (N/mm)	LJS ratio k_{FE}/k_{FE}	LJS k_{Fl} (N/mm)	LJS ratio k_{Fl}/k_{FE}	LJS k_{Ud} (N/mm)	LJS ratio k_{Ud}/k_{FE}
		93874	1.0	124491	1.33	87093	0.93
	IPB	LJS k_{FE} (N.mm)	LJS ratio k_{FE}/k_{FE}	LJS k_{Fl} (N.mm)	LJS ratio k_{Fl}/k_{FE}	LJS k_{Ud} (N.mm)	LJS ratio k_{Ud}/k_{FE}
		10.2×10^8	1.0	12.4×10^8	1.22	9.62×10^8	0.94
	Loading type	Finite Element (FE) result		Fessler's Equation		Ueda's Equation	
Y-joint	AX	LJS k_{FE} (N/mm)	LJS ratio k_{FE}/k_{FE}	LJS k_{Fl} (N/mm)	LJS ratio k_{Fl}/k_{FE}	LJS k_{Ud} (N/mm)	LJS ratio k_{Ud}/k_{FE}
		122604	1.0	134314	1.10	93348	0.76
	IPB	LJS k_{FE} (N.mm)	LJS ratio k_{FE}/k_{FE}	LJS k_{Fl} (N.mm)	LJS ratio k_{Fl}/k_{FE}	LJS k_{Ud} (N.mm)	LJS ratio k_{Ud}/k_{FE}
		12.7×10^8	1.0	12.9×10^8	1.02	9.95×10^8	0.78

in the design of practical engineering. However, the reliability of this simplification has to be assessed with cautions before its accuracy has been verified. The simplified models in Figs. 11(d) and 12(d) are then used to evaluate such reliability.

Using the above four models, the static behavior of the tubular structures as shown in Figs. 9(a) and (b) is analyzed. The 3-D finite element analyses are conducted by using the commercial software ABAQUS. For the simplified models, the analyses are completed by using the programs developed

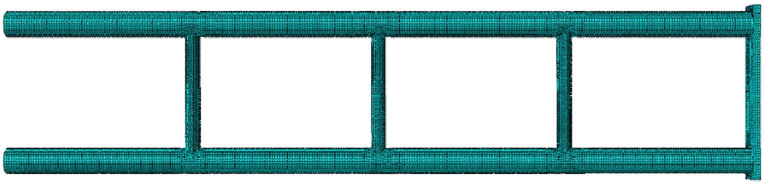

(a) 3-D finite element model

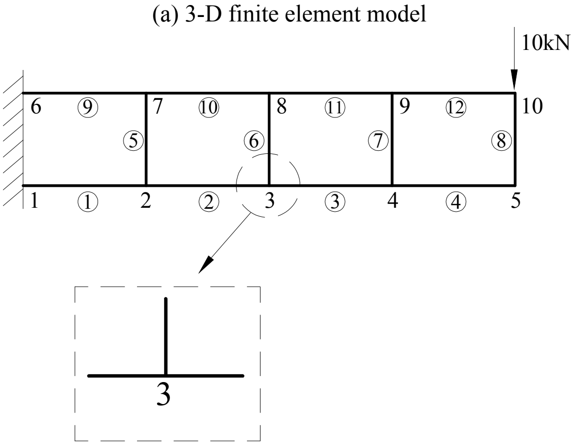

(b) Simplified frame model with rigid joint connection

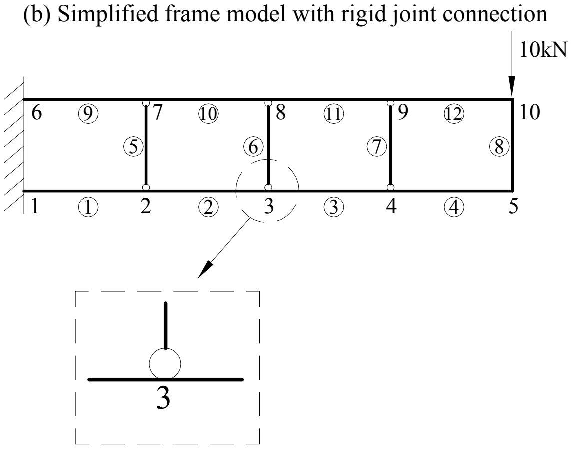

(c) Simplified frame model with hinged joint connection

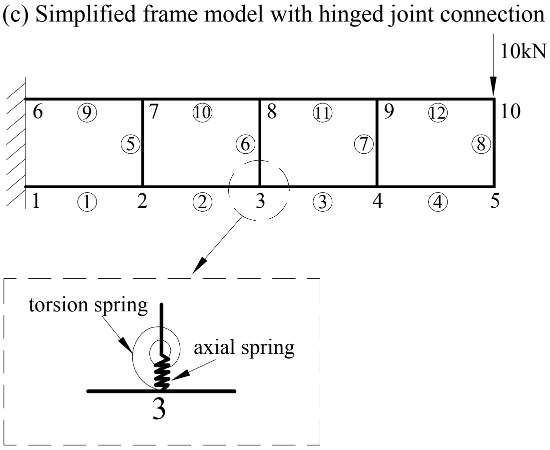

(d) Presented model

Fig. 11 Different models of tubular structures with vertical braces

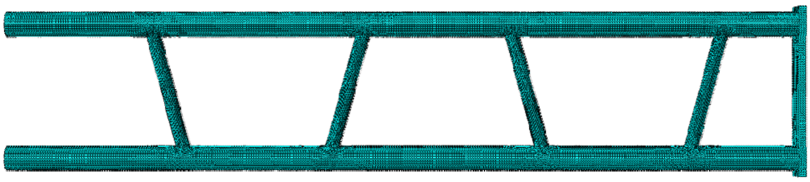

(a) 3-D finite element model

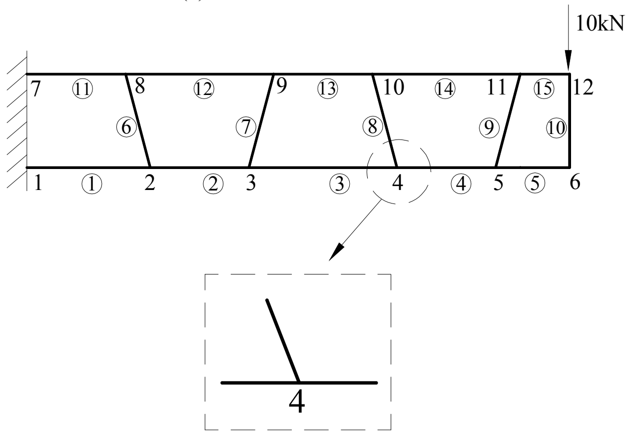

(b) Simplified frame model with rigid joint connection

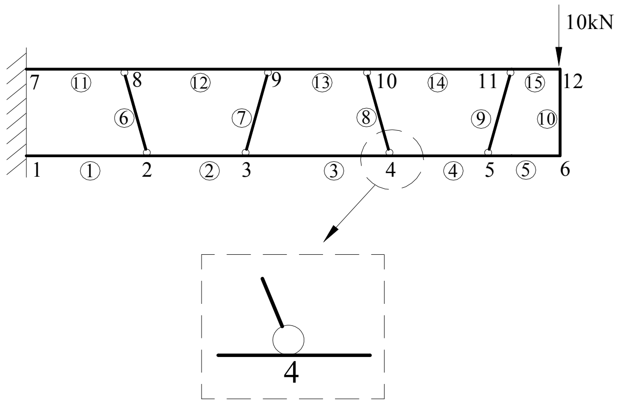

(c) Simplified frame model with hinged joint connection

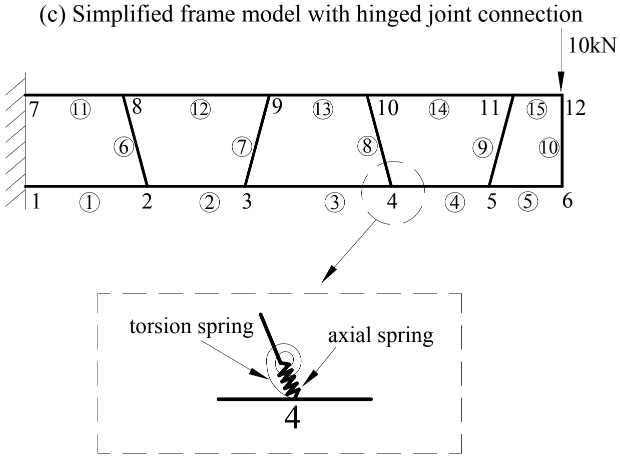

(d) Presented model

Fig. 12 Different models of tubular structures with inclined braces

by the authors based on the presented methods in this study.

The deformation of the tubular structures is described through the displacements at all the nodes. For brevity, displacements at 5 nodes (nodes 6-10 in Figs. 11(b)-(d)) for the tubular structure in Fig. 9(a) are provided. Accordingly, displacements at 6 nodes (nodes 7-12 in Figs. 12(b)-(d)) for the tubular structure with inclined braces as shown in Fig. 9(b) are used to analyze the deformation. Using the four different models, the displacements at the given points in downward direction (deflection) are plotted in Figs. 13(a)

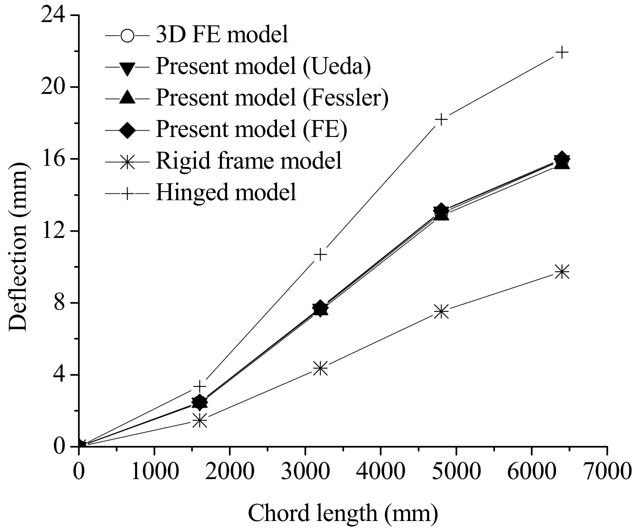

(a) Vertical braces

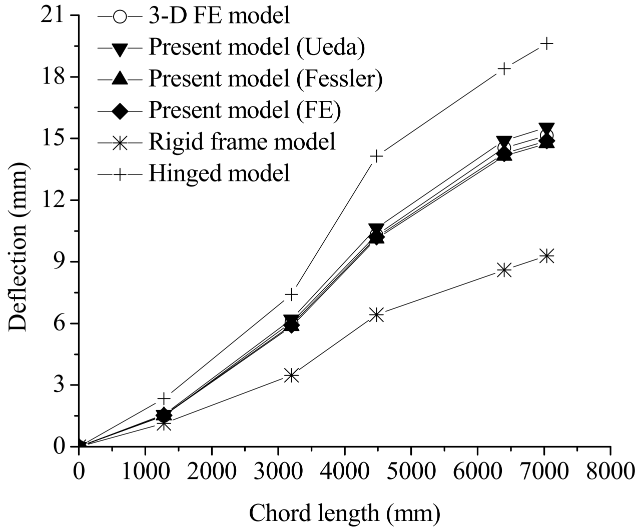

(b) Inclined braces

Fig. 13 Comparison of deflections obtained from different models

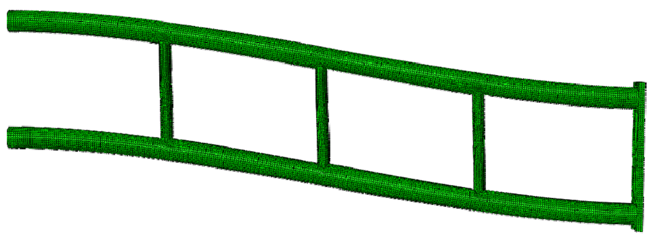

(a) 3-D finite element model

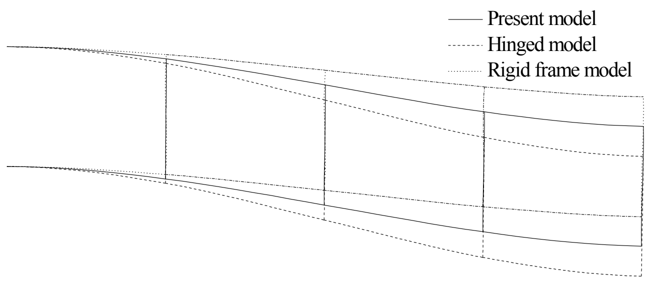

(b) Rigid frame model and presented model

Fig. 14 Deformations of tubular structure with vertical braces

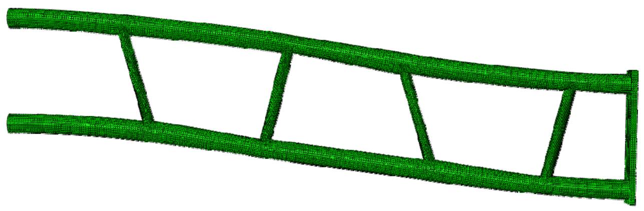

(a) 3-D finite element model

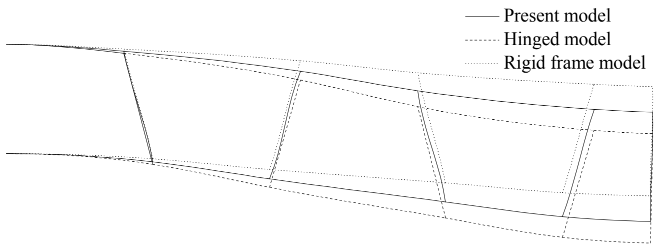

(b) Rigid frame model and presented model

Fig. 15 Deformations of tubular structure with inclined braces

and (b), in which 3-D FE model represents the results obtained from a 3-D finite element analysis by using the model in Figs. 11(a) and 12(a), Present model (Ueda) represents the results obtained from the presented simplified analytical model in this study by using Ueda's equation to calculate the LJFs at the connections, Present model (Fessler) represents the results obtained from the presented simplified analytical model in this study by using Fessler's equation to calculate the LJFs at the connections, Present model (FE) represents the results obtained from the presented simplified analytical model in this study by using 3-D finite element analyses to calculate the LJFs at the connections, Rigid Frame model represents the results obtained from the simplified rigid frame model as shown in Figs. 11(b) and 12(b), and Hinged model represents the results obtained from the simplified frame model with hinged connection between the tube braces and the top/bottom tubes as shown in Figs. 11(c) and 12(c).

From the different calculated results in Fig. 13, the following conclusions can be given: (1) The rigid frame model overestimates the stiffness of the entire structure, and it provides a lower prediction on the overall deformation of the tubular structures. (2) When the brace tubes are simplified to be hinged at their ends to the top/bottom chord tubes, the stiffness of the overall structure is under-estimated, and the deformation is much bigger than the actual result. (3) The presented simplified analytical model can provide reasonably accurate estimation for the deflection of both tubular structures. (4) Although Ueda's equation and Fessler's equation can only provide an approximate prediction on the LJFs of tubular T/Y-joints, the presented simplified analytical model by using the LJF results calculated from such equations can still produce good prediction on the deformation of the tubular structures. The above conclusions also support the reliability of the presented simplified analytical model.

Based on the calculated results from different methods, the deformations of the two tubular structures are plotted in Figs. 14 and 15. An amplification scale factor of 50 for the displacement is used in all the figures to provide a much clear view on the overall deformation of the structures. The 3-D finite element simulations are shown in Figs. 14(a) and 15(a). Figs. 14(b) and 15(b) compare the deformation of the simplified rigid frame model, hinged model and the presented analytical model considering the LJF (for accuracy, the LJF is obtained through finite element analysis). Clearly, Due to the limitation to the rotation at the connection, the deformation of the rigid frame model is much smaller, while the deformation of the hinged model is larger because of no rotation restriction at the connection between chords and braces. The simplified analytical model presented in this study, however, can produce a similar overall deformation as the 3-D finite element model.

3.3 Internal forces analysis

As the LJF has been proved to have significant effect on the overall deformation, its influence on the internal forces in the simplified frame models is also necessary to be investigated. Figs. 16(a)-(c) and Figs. 17(a)-(c) provide the detailed comparison of the internal forces between the simplified rigid frame model and the presented model (the LJF is also obtained from finite element analysis) in this study which considers the LJF at the connections. It is note here that the bending moments in Figs. 16(c) and 17(c) in each element have two values at its two connections. L means one connection with a small node number and R denotes the other connection with a big node number.

From the results illustrated in Figs. 16 and 17, it is found that the moment values of the simplified beam elements (elements 5-7 in Fig. 16 and elements 6-9 in Fig. 17) in the presented model are much smaller compared to the corresponding moment values of beam elements in the rigid frame model. As seen from Figs. 11(b)-(c) and Figs. 12(b)-(c), these beam elements are the brace members which have LJFs at the two connections to the top and the

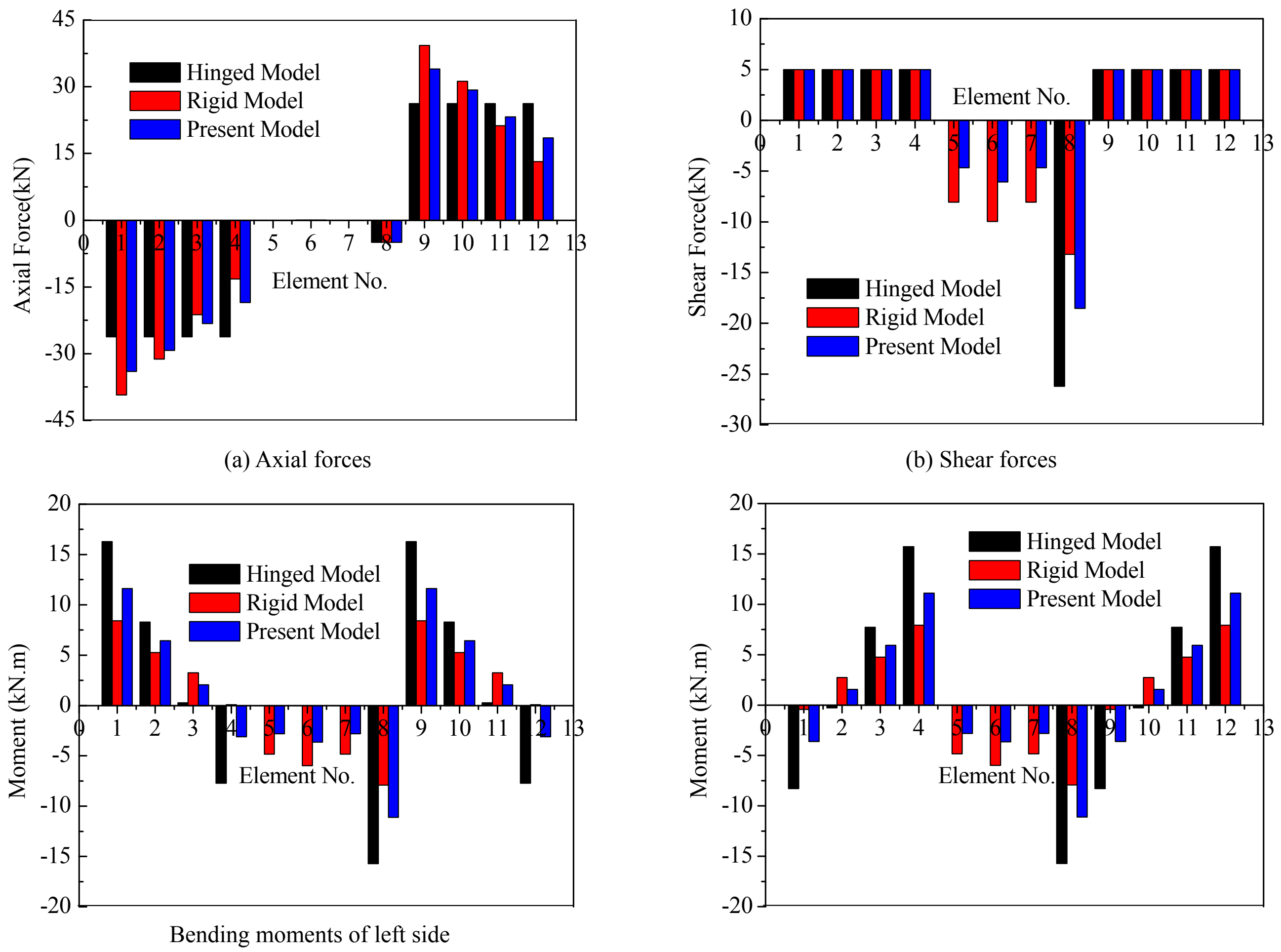

(a) Axial forces

(b) Shear forces

Bending moments of left side

(c) Bending moments of right side

Fig. 16 Internal forces in tubular structure with vertical braces

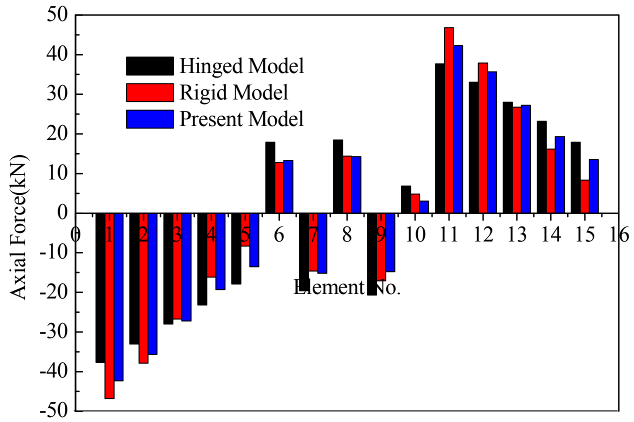

(a) Axial forces

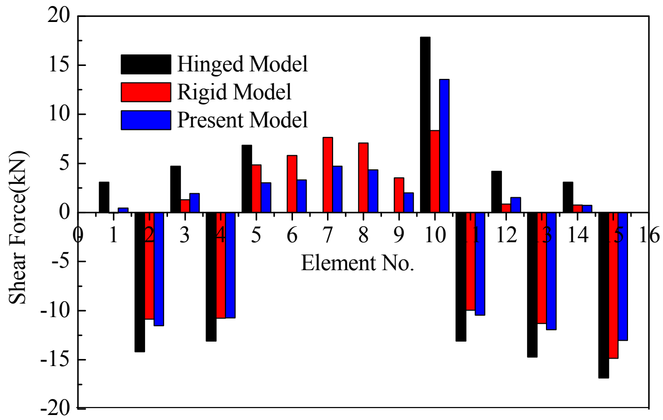

(b) Shear forces

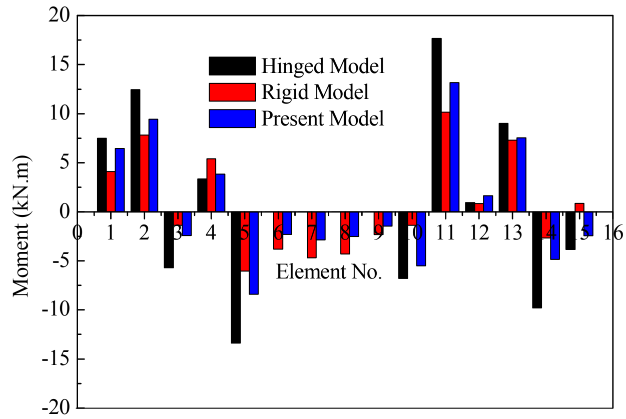

Bending moments of left side

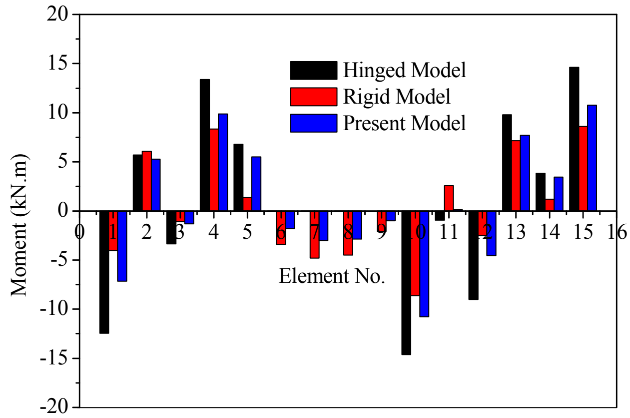

(c) Bending moments of right side

Fig. 17 Internal forces in tubular structure with inclined braces

bottom chord members. Due to such LJF, the rotation of the braces at two connections cannot be limited completely, and a portion of bending moments at the connections are released. Such moment releasing definitely reduces the moment values at the connections. Accordingly, the rotating constraints provided by the braces to the chords are weaker because the LJFs at the brace/chord connections causes the rotation between the brace and the chord to occur easily. Such weaker constraints results in the maximum bending moment of each chord member in the presented model to be bigger than that in the simplified rigid frame model. The beam element 8 in Figs. 11(b)-(c) and the beam element 10 in Figs. 12(b)-(c) in the presented model, which are rigid steel plates, have no LJFs at their two ends due to a rigid assumption at the connection, and thus they have larger values of bending moment compared to the corresponding beam elements in the rigid frame model. For shear forces, the brace members in the presented model have much lower values because of the releasing of the bending moments at the connections. For the chord members, it seems that the shear forces do not vary greatly.

4. Conclusions

This study presented a simplified analytical model for analyzing the static behaivor of tubular structures with LJF at the brace/chord connection, and the presented model has been assessed through comparing with the 3-D finite element results. From the studies in this paper, the following conclusions can be made:

- The presented model in this study has both high efficiency and good accuracy in analyzing tubular structures with LJF.
- Simplifying a tubular structure into a rigid frame model is not suitable for design purpose because such model overestimates the stiffness of the structure and provides much smaller prediction on the deformation of the entire structure. For the two tubular structures analyzed in this study, the underestimation on the deflection is about and respectively.
- Compared to the presented model, rigid frame model to simulate the two tubular structures underestimates the bending moment of the chord while overestimates the bending moment of the braces since it requires the ends of the braces (tubular joints) to resist more bending moment due to its rigid connection.
- The effect of LJF on the static performance of a tubular structure is controlled by the values of geo-metrical parameters, such as γ and β. It is easily

understood from Fessler's equation that the LJF becomes much smaller when γ is very small and β is very big. However, the presented method is still efficient to simulate such case by providing a high joint's stiffness to the stiffness matrix.

References

API (2000), Recommended practice for planning, designing and construction fixed offshore platforms; API RP2A-WSD, American Petroleum Institute, USA.

Alanjari, P., Asgarian, B. and Kia, M. (2011), "Nonlinear joint flexibility element for the modeling of jacket-type offshore platforms", *Appl. Ocean Res.*, **33**(2), 147-157.

Asgarian, B., Mokarram, V. and Alanjari, P. (2014), "Local joint flexibility equation for YT and K-type tubular joints, *Ocean Syst. Eng.*, **4**(2), 151-167.

Bouwkamp, J.G. (1996), "An improved joint model and equations for flexibility of tubular joints", *J. Petrol. Technol.*, **18**(11), 1491-1499.

Chen, B.Z., Hu, Y.R. and Tan, M.J. (1990), "Local joint flexibility of tubular joints of offshore structures", *Marine Struct.*, **3**(3), 177-197.

Chen, T. and Zhang, H. (1996), "Stress analysis of spatial frames with consideration of local flexibility of multiplanar tubular joint", *Eng. Struct.*, **18**(6), 465-471.

Fessler, H., Mockford, P.B. and Webster, J.J. (1986), "Parametric equations for the flexibility matrix of single brace tubular joint in offshore structures", *Proceedings of the Institution of Civil Engineers*, **81**(4), 659-673.

Gao, F., Hu, B. and Zhu, H.P. (2013), "Parametric equations to predict LJF of completely overlapped tubular joints under lap brace axial loading", *J. Constr. Steel Res.*, **89**, 284-292.

Gao, F., Hu, B. and Zhu, H.P. (2014), "Local joint flexibility of completely overlapped tubular joints under in-plane bending", *J. Constr. Steel Res.*, **99**, 1-9.

Gou, H., Pu, Q., Zhou, Y. and Yu, H. (2015), "Arch-to-beam rigidity analysis for V-shaped rigid frame composite arch bridges", *Steel Compos. Struct.*, *Int. J.*, **19**(2), 405-416.

Hu, Y.R., Chen, B.Z. and Tan, M.J. (1993), "An equivalent element representing local flexibility of tubular joints in structural analysis of offshore platforms", *Comput. Struct.*, **47**(6), 957-969.

Jia, L.J. and Chen, Y.Y. (2014), "Evaluation of elastic in-plane flexural rigidity of unstiffened multiplanar CHS X-joints", *Int. J. Steel Struct.*, **14**(1), 23-30.

Liu, H., Chen, Z., Xu, S. and Bu, Y. (2015), "Structural behavior of aluminum reticulated shell structures considering semi-rigid and skin effect", *Steel Compos. Struct.*, *Int. J.*, **54**(1), 121-133.

Mirtaheri, M., Ali Zakeri, H., Alanjari, P. and Amin Assareh, M. (2009), "Effect of joint flexibility on overall behavior of jacket type offshore platforms", *Am. J. Eng. Appl. Sci.*, **2**(1), 25-30.

Nguyen, P.C. and Kim, S.E. (2016), "Advanced analysis for planar steel frames with semi-rigid connections using plastic-zone method", *Steel Compos. Struct.*, *Int. J.*, **21**(5), 1121-1144.

Qiu, G.Z., Gong, J.H. and Zhao, J.C. (2011), "Parametric formulae for axial stiffness of CHS X-joints subjected to brace axial tension", *J. Zhejiang Univ.-Sci. A* (*Appl. Phys. Eng.*), **12**(2), 121-130.

Qiu, G.Z. and Zhao, J.C. (2009), "Analysis and calculation of axial stiffness of tubular X-joints under compression on braces", *J. Shanghai Jiaotong Univ.* (*Science Ed.*), **14**(4), 410-417.

Sagiroglu, A. and Aydin, A.C. (2015), "Design and analysis of non-linear space frames with semi-rigid connections", *Steel Compos. Struct.*, *Int. J.*, **18**(6), 1405-1421.

Ueda, Y., Rashed, S.M.H. and Nakacho, K. (1990), "An improved joint model and equations for flexibility of tubular joints", *J. Offshore Mech. Arctic Eng.*, **112**(2), 157-168.

Wang, W. and Chen, Y.Y. (2005), "Modelling and classification of tubular joint rigidity and its effect on the global response of CHS lattice girders", *Struct. Eng. Mech.*, *Int. J.*, **21**(6), 677-698.

Yang, L.X., Chen, T.Y. and Wu, S.Y. (1990), "Local flexibility behavior of tubular joints and its effect on global analysis of tubular structures", *China Ocean Eng.*, **4**(4), 371-384.

BU